Observation of B_s^0-$\bar{B}_s^0$ Oscillations

A. Abulencia,[23] J. Adelman,[13] T. Affolder,[10] T. Akimoto,[55] M.G. Albrow,[16] D. Ambrose,[16] S. Amerio,[43] D. Amidei,[34] A. Anastassov,[52] K. Anikeev,[16] A. Annovi,[18] J. Antos,[1] M. Aoki,[55] G. Apollinari,[16] J.-F. Arguin,[33] T. Arisawa,[57] A. Artikov,[14] W. Ashmanskas,[16] A. Attal,[8] F. Azfar,[42] P. Azzi-Bacchetta,[43] P. Azzurri,[46] N. Bacchetta,[43] W. Badgett,[16] A. Barbaro-Galtieri,[28] V.E. Barnes,[48] B.A. Barnett,[24] S. Baroiant,[7] V. Bartsch,[30] G. Bauer,[32] F. Bedeschi,[46] S. Behari,[24] S. Belforte,[54] G. Bellettini,[46] J. Bellinger,[59] A. Belloni,[32] D. Benjamin,[15] A. Beretvas,[16] J. Beringer,[28] T. Berry,[29] A. Bhatti,[50] M. Binkley,[16] D. Bisello,[43] R.E. Blair,[2] C. Blocker,[6] B. Blumenfeld,[24] A. Bocci,[15] A. Bodek,[49] V. Boisvert,[49] G. Bolla,[48] A. Bolshov,[32] D. Bortoletto,[48] J. Boudreau,[47] A. Boveia,[10] B. Brau,[10] L. Brigliadori,[5] C. Bromberg,[35] E. Brubaker,[13] J. Budagov,[14] H.S. Budd,[49] S. Budd,[23] S. Budroni,[46] K. Burkett,[16] G. Busetto,[43] P. Bussey,[20] K. L. Byrum,[2] S. Cabrera,[15] M. Campanelli,[19] M. Campbell,[34] F. Canelli,[16] A. Canepa,[48] S. Carrillo,[17] D. Carlsmith,[59] R. Carosi,[46] S. Carron,[33] B. Casal,[11] M. Casarsa,[54] A. Castro,[5] P. Catastini,[46] D. Cauz,[54] M. Cavalli-Sforza,[3] A. Cerri,[28] L. Cerrito,[30] S.H. Chang,[27] Y.C. Chen,[1] M. Chertok,[7] G. Chiarelli,[46] G. Chlachidze,[14] F. Chlebana,[16] I. Cho,[27] K. Cho,[27] D. Chokheli,[14] J.P. Chou,[21] G. Choudalakis,[32] S.H. Chuang,[59] K. Chung,[12] W.H. Chung,[59] Y.S. Chung,[49] M. Ciljak,[46] C.I. Ciobanu,[23] M.A. Ciocci,[46] A. Clark,[19] D. Clark,[6] M. Coca,[15] G. Compostella,[43] M.E. Convery,[50] J. Conway,[7] B. Cooper,[35] K. Copic,[34] M. Cordelli,[18] G. Cortiana,[43] F. Crescioli,[46] C. Cuenca Almenar,[7] J. Cuevas,[11] R. Culbertson,[16] J.C. Cully,[34] D. Cyr,[59] S. DaRonco,[43] S. D'Auria,[20] T. Davies,[20] M. D'Onofrio,[3] D. Dagenhart,[6] P. de Barbaro,[49] S. De Cecco,[51] A. Deisher,[28] G. De Lentdecker,[49] M. Dell'Orso,[46] F. Delli Paoli,[43] L. Demortier,[50] J. Deng,[15] M. Deninno,[5] D. De Pedis,[51] P.F. Derwent,[16] G.P. Di Giovanni,[44] C. Dionisi,[51] B. Di Ruzza,[54] J.R. Dittmann,[4] P. DiTuro,[52] C. Dörr,[25] S. Donati,[46] M. Donega,[19] P. Dong,[8] J. Donini,[43] T. Dorigo,[43] S. Dube,[52] J. Efron,[39] R. Erbacher,[7] D. Errede,[23] S. Errede,[23] R. Eusebi,[16] H.C. Fang,[28] S. Farrington,[29] I. Fedorko,[46] W.T. Fedorko,[13] R.G. Feild,[60] M. Feindt,[25] J.P. Fernandez,[31] R. Field,[17] G. Flanagan,[48] A. Foland,[21] S. Forrester,[7] G.W. Foster,[16] M. Franklin,[21] J.C. Freeman,[28] H. J. Frisch,[13] I. Furic,[13] M. Gallinaro,[50] J. Galyardt,[12] J.E. Garcia,[46] F. Garberson,[10] A.F. Garfinkel,[48] C. Gay,[60] H. Gerberich,[23] D. Gerdes,[34] S. Giagu,[51] P. Giannetti,[46] A. Gibson,[28] K. Gibson,[47] J.L. Gimmell,[49] C. Ginsburg,[16] N. Giokaris,[14] M. Giordani,[54] P. Giromini,[18] M. Giunta,[46] G. Giurgiu,[12] V. Glagolev,[14] D. Glenzinski,[16] M. Gold,[37] N. Goldschmidt,[17] J. Goldstein,[42] G. Gomez,[11] G. Gomez-Ceballos,[11] M. Goncharov,[53] O. González,[31] I. Gorelov,[37] A.T. Goshaw,[15] K. Goulianos,[50] A. Gresele,[43] M. Griffiths,[29] S. Grinstein,[21] C. Grosso-Pilcher,[13] R.C. Group,[17] U. Grundler,[23] J. Guimaraes da Costa,[21] Z. Gunay-Unalan,[35] C. Haber,[28] K. Hahn,[32] S.R. Hahn,[16] E. Halkiadakis,[52] A. Hamilton,[33] B.-Y. Han,[49] J.Y. Han,[49] R. Handler,[59] F. Happacher,[18] K. Hara,[55] M. Hare,[56] S. Harper,[42] R.F. Harr,[58] R.M. Harris,[16] M. Hartz,[47] K. Hatakeyama,[50] J. Hauser,[8] A. Heijboer,[45] B. Heinemann,[29] J. Heinrich,[45] C. Henderson,[32] M. Herndon,[59] J. Heuser,[25] D. Hidas,[15] C.S. Hill,[10] D. Hirschbuehl,[25] A. Hocker,[16] A. Holloway,[21] S. Hou,[1] M. Houlden,[29] S.-C. Hsu,[9] B.T. Huffman,[42] R.E. Hughes,[39] U. Husemann,[60] J. Huston,[35] J. Incandela,[10] G. Introzzi,[46] M. Iori,[51] Y. Ishizawa,[55] A. Ivanov,[7] B. Iyutin,[32] E. James,[16] D. Jang,[52] B. Jayatilaka,[34] D. Jeans,[51] H. Jensen,[16] E.J. Jeon,[27] S. Jindariani,[17] M. Jones,[48] K.K. Joo,[27] S.Y. Jun,[12] J.E. Jung,[27] T.R. Junk,[23] T. Kamon,[53] P.E. Karchin,[58] Y. Kato,[41] Y. Kemp,[25] R. Kephart,[16] U. Kerzel,[25] V. Khotilovich,[53] B. Kilminster,[39] D.H. Kim,[27] H.S. Kim,[27] J.E. Kim,[27] M.J. Kim,[12] S.B. Kim,[27] S.H. Kim,[55] Y.K. Kim,[13] N. Kimura,[55] L. Kirsch,[6] S. Klimenko,[17] M. Klute,[32] B. Knuteson,[32] B.R. Ko,[15] K. Kondo,[57] D.J. Kong,[27] J. Konigsberg,[17] A. Korytov,[17] A.V. Kotwal,[15] A. Kovalev,[45] A.C. Kraan,[45] J. Kraus,[23] I. Kravchenko,[32] M. Kreps,[25] J. Kroll,[45] N. Krumnack,[4] M. Kruse,[15] V. Krutelyov,[10] T. Kubo,[55] S. E. Kuhlmann,[2] T. Kuhr,[25] Y. Kusakabe,[57] S. Kwang,[13] A.T. Laasanen,[48] S. Lai,[33] S. Lami,[46] S. Lammel,[16] M. Lancaster,[30] R.L. Lander,[7] K. Lannon,[39] A. Lath,[52] G. Latino,[46] I. Lazzizzera,[43] T. LeCompte,[2] J. Lee,[49] J. Lee,[27] Y.J. Lee,[27] S.W. Lee,[53] R. Lefèvre,[3] N. Leonardo,[32] S. Leone,[46] S. Levy,[13] J.D. Lewis,[16] C. Lin,[60] C.S. Lin,[16] M. Lindgren,[16] E. Lipeles,[9] T.M. Liss,[23] A. Lister,[7] D.O. Litvintsev,[16] T. Liu,[16] N.S. Lockyer,[45] A. Loginov,[36] M. Loreti,[43] P. Loverre,[51] R.-S. Lu,[1] D. Lucchesi,[43] P. Lujan,[28] P. Lukens,[16] G. Lungu,[17] L. Lyons,[42] J. Lys,[28] R. Lysak,[1] E. Lytken,[48] P. Mack,[25] D. MacQueen,[33] R. Madrak,[16] K. Maeshima,[16] K. Makhoul,[32] T. Maki,[22] P. Maksimovic,[24] S. Malde,[42] G. Manca,[29] F. Margaroli,[5] R. Marginean,[16] C. Marino,[25] C.P. Marino,[23] A. Martin,[60] M. Martin,[24] V. Martin,[20] M. Martínez,[3] T. Maruyama,[55] P. Mastrandrea,[51] T. Masubuchi,[55] H. Matsunaga,[55] M.E. Mattson,[58] R. Mazini,[33] P. Mazzanti,[5] K.S. McFarland,[49] P. McIntyre,[53] R. McNulty,[29] A. Mehta,[29] P. Mehtala,[22] S. Menzemer,[11] A. Menzione,[46] P. Merkel,[48] C. Mesropian,[50] A. Messina,[51] T. Miao,[16] N. Miladinovic,[6] J. Miles,[32] R. Miller,[35] C. Mills,[10] M. Milnik,[25] A. Mitra,[1] G. Mitselmakher,[17] A. Miyamoto,[26] S. Moed,[19] N. Moggi,[5] B. Mohr,[8]

R. Moore,[16] M. Morello,[46] P. Movilla Fernandez,[28] J. Mülmenstädt,[28] A. Mukherjee,[16] Th. Muller,[25] R. Mumford,[24] P. Murat,[16] J. Nachtman,[16] A. Nagano,[55] J. Naganoma,[57] S. Nahn,[32] I. Nakano,[40] A. Napier,[56] V. Necula,[17] C. Neu,[45] M.S. Neubauer,[9] J. Nielsen,[28] T. Nigmanov,[47] L. Nodulman,[2] O. Norniella,[3] E. Nurse,[30] S.H. Oh,[15] Y.D. Oh,[27] I. Oksuzian,[17] T. Okusawa,[41] R. Oldeman,[29] R. Orava,[22] K. Osterberg,[22] C. Pagliarone,[46] E. Palencia,[11] V. Papadimitriou,[16] A.A. Paramonov,[13] B. Parks,[39] S. Pashapour,[33] J. Patrick,[16] G. Pauletta,[54] M. Paulini,[12] C. Paus,[32] D.E. Pellett,[7] A. Penzo,[54] T.J. Phillips,[15] G. Piacentino,[46] J. Piedra,[44] L. Pinera,[17] K. Pitts,[23] C. Plager,[8] L. Pondrom,[59] X. Portell,[3] O. Poukhov,[14] N. Pounder,[42] F. Prokoshin,[14] A. Pronko,[16] J. Proudfoot,[2] F. Ptochos,[18] G. Punzi,[46] J. Pursley,[24] J. Rademacker,[42] A. Rahaman,[47] N. Ranjan,[48] S. Rappoccio,[21] B. Reisert,[16] V. Rekovic,[37] P. Renton,[42] M. Rescigno,[51] S. Richter,[25] F. Rimondi,[5] L. Ristori,[46] A. Robson,[20] T. Rodrigo,[11] E. Rogers,[23] S. Rolli,[56] R. Roser,[16] M. Rossi,[54] R. Rossin,[17] A. Ruiz,[11] J. Russ,[12] V. Rusu,[13] H. Saarikko,[22] S. Sabik,[33] A. Safonov,[53] W.K. Sakumoto,[49] G. Salamanna,[51] O. Saltó,[3] D. Saltzberg,[8] C. Sánchez,[3] L. Santi,[54] S. Sarkar,[51] L. Sartori,[46] K. Sato,[16] P. Savard,[33] A. Savoy-Navarro,[44] T. Scheidle,[25] P. Schlabach,[16] E.E. Schmidt,[16] M.P. Schmidt,[60] M. Schmitt,[38] T. Schwarz,[7] L. Scodellaro,[11] A.L. Scott,[10] A. Scribano,[46] F. Scuri,[46] A. Sedov,[48] S. Seidel,[37] Y. Seiya,[41] A. Semenov,[14] L. Sexton-Kennedy,[16] A. Sfyrla,[19] M.D. Shapiro,[28] T. Shears,[29] P.F. Shepard,[47] D. Sherman,[21] M. Shimojima,[55] M. Shochet,[13] Y. Shon,[59] I. Shreyber,[36] A. Sidoti,[46] P. Sinervo,[33] A. Sisakyan,[14] J. Sjolin,[42] A.J. Slaughter,[16] J. Slaunwhite,[39] K. Sliwa,[56] J.R. Smith,[7] F.D. Snider,[16] R. Snihur,[33] M. Soderberg,[34] A. Soha,[7] S. Somalwar,[52] V. Sorin,[35] J. Spalding,[16] F. Spinella,[46] T. Spreitzer,[33] P. Squillacioti,[46] M. Stanitzki,[60] A. Staveris-Polykalas,[46] R. St. Denis,[20] B. Stelzer,[8] O. Stelzer-Chilton,[42] D. Stentz,[38] J. Strologas,[37] D. Stuart,[10] J.S. Suh,[27] A. Sukhanov,[17] H. Sun,[56] T. Suzuki,[55] A. Taffard,[23] R. Takashima,[40] Y. Takeuchi,[55] K. Takikawa,[55] M. Tanaka,[2] R. Tanaka,[40] M. Tecchio,[34] P.K. Teng,[1] K. Terashi,[50] J. Thom,[16] A.S. Thompson,[20] E. Thomson,[45] P. Tipton,[60] V. Tiwari,[12] S. Tkaczyk,[16] D. Toback,[53] S. Tokar,[14] K. Tollefson,[35] T. Tomura,[55] D. Tonelli,[46] S. Torre,[18] D. Torretta,[16] S. Tourneur,[44] W. Trischuk,[33] R. Tsuchiya,[57] S. Tsuno,[40] N. Turini,[46] F. Ukegawa,[55] T. Unverhau,[20] S. Uozumi,[55] D. Usynin,[45] S. Vallecorsa,[19] N. van Remortel,[22] A. Varganov,[34] E. Vataga,[37] F. Vázquez,[17] G. Velev,[16] G. Veramendi,[23] V. Veszpremi,[48] R. Vidal,[16] I. Vila,[11] R. Vilar,[11] T. Vine,[30] I. Vollrath,[33] I. Volobouev,[28] G. Volpi,[46] F. Würthwein,[9] P. Wagner,[53] R.G. Wagner,[2] R.L. Wagner,[16] J. Wagner,[25] W. Wagner,[25] R. Wallny,[8] S.M. Wang,[1] A. Warburton,[33] S. Waschke,[20] D. Waters,[30] M. Weinberger,[53] W.C. Wester III,[16] B. Whitehouse,[56] D. Whiteson,[45] A.B. Wicklund,[2] E. Wicklund,[16] G. Williams,[33] H.H. Williams,[45] P. Wilson,[16] B.L. Winer,[39] P. Wittich,[16] S. Wolbers,[16] C. Wolfe,[13] T. Wright,[34] X. Wu,[19] S.M. Wynne,[29] A. Yagil,[16] K. Yamamoto,[41] J. Yamaoka,[52] T. Yamashita,[40] C. Yang,[60] U.K. Yang,[13] Y.C. Yang,[27] W.M. Yao,[28] G.P. Yeh,[16] J. Yoh,[16] K. Yorita,[13] T. Yoshida,[41] G.B. Yu,[49] I. Yu,[27] S.S. Yu,[16] J.C. Yun,[16] L. Zanello,[51] A. Zanetti,[54] I. Zaw,[21] X. Zhang,[23] J. Zhou,[52] and S. Zucchelli[5]

(CDF Collaboration)

[1]*Institute of Physics, Academia Sinica, Taipei, Taiwan 11529, Republic of China*
[2]*Argonne National Laboratory, Argonne, Illinois 60439*
[3]*Institut de Fisica d'Altes Energies, Universitat Autonoma de Barcelona, E-08193, Bellaterra (Barcelona), Spain*
[4]*Baylor University, Waco, Texas 76798*
[5]*Istituto Nazionale di Fisica Nucleare, University of Bologna, I-40127 Bologna, Italy*
[6]*Brandeis University, Waltham, Massachusetts 02254*
[7]*University of California, Davis, Davis, California 95616*
[8]*University of California, Los Angeles, Los Angeles, California 90024*
[9]*University of California, San Diego, La Jolla, California 92093*
[10]*University of California, Santa Barbara, Santa Barbara, California 93106*
[11]*Instituto de Fisica de Cantabria, CSIC-University of Cantabria, 39005 Santander, Spain*
[12]*Carnegie Mellon University, Pittsburgh, PA 15213*
[13]*Enrico Fermi Institute, University of Chicago, Chicago, Illinois 60637*
[14]*Joint Institute for Nuclear Research, RU-141980 Dubna, Russia*
[15]*Duke University, Durham, North Carolina 27708*
[16]*Fermi National Accelerator Laboratory, Batavia, Illinois 60510*
[17]*University of Florida, Gainesville, Florida 32611*
[18]*Laboratori Nazionali di Frascati, Istituto Nazionale di Fisica Nucleare, I-00044 Frascati, Italy*
[19]*University of Geneva, CH-1211 Geneva 4, Switzerland*
[20]*Glasgow University, Glasgow G12 8QQ, United Kingdom*
[21]*Harvard University, Cambridge, Massachusetts 02138*
[22]*Division of High Energy Physics, Department of Physics,*
University of Helsinki and Helsinki Institute of Physics, FIN-00014, Helsinki, Finland
[23]*University of Illinois, Urbana, Illinois 61801*

[24] The Johns Hopkins University, Baltimore, Maryland 21218
[25] Institut für Experimentelle Kernphysik, Universität Karlsruhe, 76128 Karlsruhe, Germany
[26] High Energy Accelerator Research Organization (KEK), Tsukuba, Ibaraki 305, Japan
[27] Center for High Energy Physics: Kyungpook National University, Taegu 702-701, Korea; Seoul National University, Seoul 151-742, Korea; and SungKyunKwan University, Suwon 440-746, Korea
[28] Ernest Orlando Lawrence Berkeley National Laboratory, Berkeley, California 94720
[29] University of Liverpool, Liverpool L69 7ZE, United Kingdom
[30] University College London, London WC1E 6BT, United Kingdom
[31] Centro de Investigaciones Energeticas Medioambientales y Tecnologicas, E-28040 Madrid, Spain
[32] Massachusetts Institute of Technology, Cambridge, Massachusetts 02139
[33] Institute of Particle Physics: McGill University, Montréal, Canada H3A 2T8; and University of Toronto, Toronto, Canada M5S 1A7
[34] University of Michigan, Ann Arbor, Michigan 48109
[35] Michigan State University, East Lansing, Michigan 48824
[36] Institution for Theoretical and Experimental Physics, ITEP, Moscow 117259, Russia
[37] University of New Mexico, Albuquerque, New Mexico 87131
[38] Northwestern University, Evanston, Illinois 60208
[39] The Ohio State University, Columbus, Ohio 43210
[40] Okayama University, Okayama 700-8530, Japan
[41] Osaka City University, Osaka 588, Japan
[42] University of Oxford, Oxford OX1 3RH, United Kingdom
[43] University of Padova, Istituto Nazionale di Fisica Nucleare, Sezione di Padova-Trento, I-35131 Padova, Italy
[44] LPNHE, Universite Pierre et Marie Curie/IN2P3-CNRS, UMR7585, Paris, F-75252 France
[45] University of Pennsylvania, Philadelphia, Pennsylvania 19104
[46] Istituto Nazionale di Fisica Nucleare Pisa, Universities of Pisa, Siena and Scuola Normale Superiore, I-56127 Pisa, Italy
[47] University of Pittsburgh, Pittsburgh, Pennsylvania 15260
[48] Purdue University, West Lafayette, Indiana 47907
[49] University of Rochester, Rochester, New York 14627
[50] The Rockefeller University, New York, New York 10021
[51] Istituto Nazionale di Fisica Nucleare, Sezione di Roma 1, University of Rome "La Sapienza," I-00185 Roma, Italy
[52] Rutgers University, Piscataway, New Jersey 08855
[53] Texas A&M University, College Station, Texas 77843
[54] Istituto Nazionale di Fisica Nucleare, University of Trieste/ Udine, Italy
[55] University of Tsukuba, Tsukuba, Ibaraki 305, Japan
[56] Tufts University, Medford, Massachusetts 02155
[57] Waseda University, Tokyo 169, Japan
[58] Wayne State University, Detroit, Michigan 48201
[59] University of Wisconsin, Madison, Wisconsin 53706
[60] Yale University, New Haven, Connecticut 06520

We report the observation of B_s^0-$\bar{B}_s^0$ oscillations from a time-dependent measurement of the B_s^0-$\bar{B}_s^0$ oscillation frequency Δm_s. Using a data sample of 1 fb^{-1} of $p\bar{p}$ collisions at $\sqrt{s} = 1.96$ TeV collected with the CDF II detector at the Fermilab Tevatron, we find signals of 5600 fully reconstructed hadronic B_s decays, 3100 partially reconstructed hadronic B_s decays, and 61 500 partially reconstructed semileptonic B_s decays. We measure the probability as a function of proper decay time that the B_s decays with the same, or opposite, flavor as the flavor at production, and we find a signal for B_s^0-$\bar{B}_s^0$ oscillations. The probability that random fluctuations could produce a comparable signal is 8×10^{-8}, which exceeds 5σ significance. We measure $\Delta m_s = 17.77 \pm 0.10$ (stat) ± 0.07 (syst) ps^{-1} and extract $|V_{td}/V_{ts}| = 0.2060 \pm 0.0007$ (exp) $^{+0.0081}_{-0.0060}$ (theor).

PACS numbers: 14.40.Nd, 12.15.Ff, 12.15.Hh, 13.20.He

Since the first observation of particle-antiparticle transformations in neutral B mesons in 1987 [1], the determination of the B_s^0-$\bar{B}_s^0$ oscillation frequency Δm_s from a time-dependent measurement of B_s^0-$\bar{B}_s^0$ oscillations has been a major objective of experimental particle physics [2]. This frequency can be used to extract the magnitude of V_{ts}, one of the nine elements of the Cabibbo-Kobayashi-Maskawa (CKM) matrix [3]. Recently, we reported [4] the strongest evidence to date of the direct observation of B_s^0-$\bar{B}_s^0$ oscillations. That analysis used 1 fb^{-1} of data collected with the CDF II detector at the Fermilab Tevatron, and the probability that random fluctuations would produce a comparable signal

was 0.2%, corresponding to 3σ signal significance. This level of significance is insufficient to claim a firm observation, however, under the oscillation hypothesis we determined $\Delta m_s = 17.31\ ^{+0.33}_{-0.18}\ (\text{stat})\ \pm 0.07\ (\text{syst})\,\text{ps}^{-1}$. In this Letter we report an update of this measurement that uses the same data set with an improved analysis and reduces this probability to 8×10^{-8} ($> 5\sigma$), yielding the first definitive observation of time-dependent B_s^0-$\bar{B}_s^0$ oscillations.

We improve the analysis in Ref. [4] by increasing the B_s signal yield and improving the performance of the methods used to identify the flavor (b or $\bar{b}$) of the B_s at production. The previous analysis used B_s decays in hadronic ($\bar{B}_s^0 \to D_s^+\pi^-$, $D_s^+\pi^-\pi^+\pi^-$) and semileptonic ($\bar{B}_s^0 \to D_s^{+(*)}\ell^-\bar{\nu}_\ell$, $\ell = e$ or μ) decay modes [5]. We used $D_s^+ \to \phi\pi^+$, $\bar{K}^*(892)^0K^+$, and $\pi^+\pi^-\pi^+$, with $\phi \to K^+K^-$ and $\bar{K}^{*0} \to K^-\pi^+$. Several improvements lead to increased signal yields. We use particle identification techniques to find kaons from D_s meson decays, allowing us to relax kinematic selection requirements on the D_s decay products. This results in increased efficiency for reconstructing the D_s while maintaining excellent signal to background. In the hadronic channels, we employ an artificial neural network (ANN) to improve candidate selection resulting in larger signal yields at similar or smaller background levels. The ANN selection makes it possible to use the additional decay sequence $\bar{B}_s^0 \to D_s^+\pi^-\pi^+\pi^-$, with $D_s^+ \to \pi^+\pi^-\pi^+$, as well. We add significant statistics using partially reconstructed hadronic decays in which a photon or π^0 is missing: $\bar{B}_s^0 \to D_s^{*+}\pi^-$, $D_s^{*+} \to D_s^+\gamma/\pi^0$ and $\bar{B}_s^0 \to D_s^+\rho^-$, $\rho^- \to \pi^-\pi^0$, with $D_s^+ \to \phi\pi^+$. Finally ANNs are used to enhance the performance of the methods used to identify the flavor of the B_s at production. With all these improvements, the effective statistical size of our data sample is increased by a factor of 2.5.

The CDF II detector [6] consists of a magnetic spectrometer surrounded by electromagnetic and hadronic calorimeters and muon detectors. The key components for this measurement are listed below. Precision determination of the decay point is provided by a seven-layer double-sided silicon-strip detector and a single-sided layer of silicon mounted directly on the beampipe at an average radius of 1.5 cm. A 96-layer drift chamber is used for both precision tracking and dE/dx particle identification. Time-of-flight (TOF) counters surrounding the drift chamber are used to identify low-momentum charged kaons. A three-level trigger system selects, in real time, $p\bar{p}$ collisions containing charm and bottom hadrons by exploiting the kinematics of production and decay, and the long lifetimes of D and B mesons. A crucial component of the trigger system for this measurement is the Silicon Vertex Trigger, which makes it possible to collect our large sample of B_s mesons in the fully or partially reconstructed hadronic decay modes, giving CDF unique sensitivity to B_s oscillations.

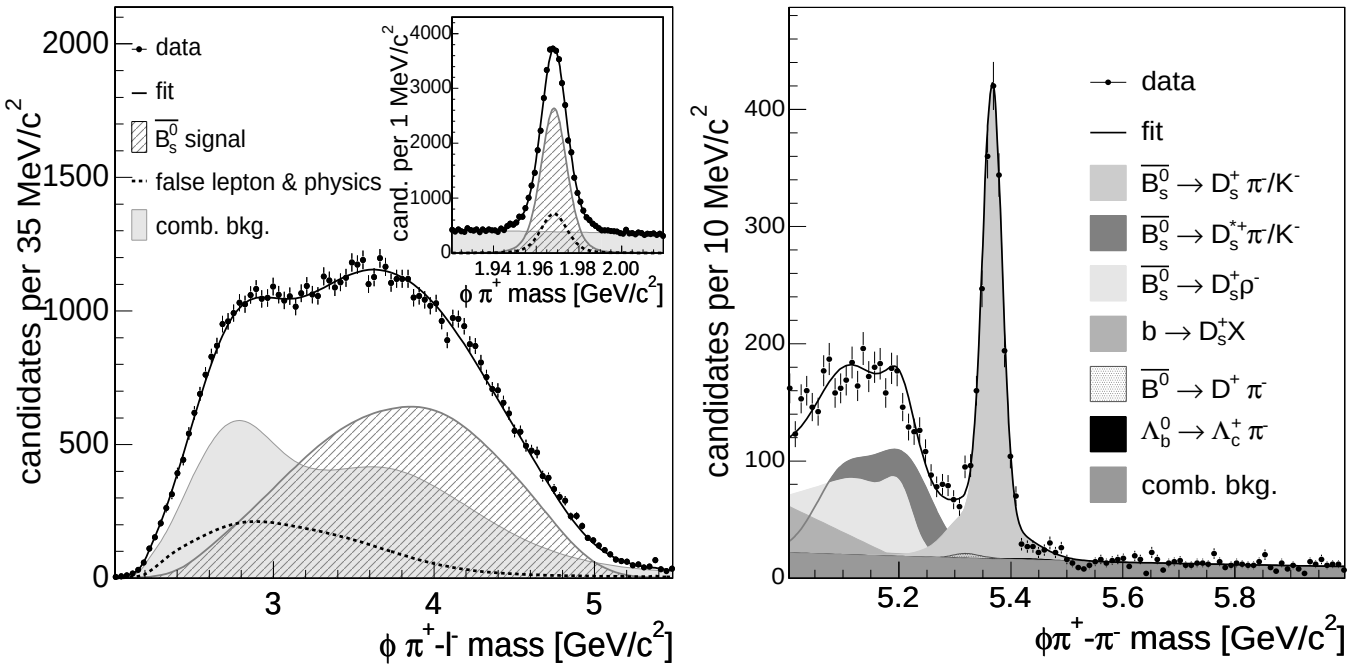

FIG. 1: (Left panel) The invariant mass distributions for the $D_s^+(\phi\pi^+)$ candidates [inset] and the $\ell^- D_s^+(\phi\pi^+)$ pairs. The contribution labelled "false lepton & physics" refers to backgrounds from hadrons mimicking the lepton signature combined with real D_s mesons and physics backgrounds such as $B^0 \to D_s^+D^-$, $D_s^+ \to \phi\pi^+, D^- \to \ell^- X$. (Right panel) The invariant mass distribution for $\bar{B}_s^0 \to D_s^+(\phi\pi^+)\pi^-$ decays including the contributions from $\bar{B}_s^0 \to D_s^{*+}\pi^-$ and $\bar{B}_s^0 \to D_s^+\rho^-$. In this panel, signal contributions are drawn added on top of the combinatorial background.

To reconstruct $\bar{B}_s^0$ candidates, we first select D_s^+ candidates. These D_s^+ candidates are combined with one or three additional charged particles to form $D_s^+\ell^-$, $D_s^+\pi^-$, or $D_s^+\pi^-\pi^+\pi^-$ candidates. In the previous analysis, we reduced combinatorial backgrounds by applying requirements on selection quantities such as the minimum p_T [7] of the $\bar{B}_s^0$ and its decay products, and the quality of the reconstructed $\bar{B}_s^0$ and D_s^+ decay points and their displacement from the $p\bar{p}$ collision position. In this analysis, we add a kaon identification likelihood formed from TOF and dE/dx information. For decay modes with kaons in the final state, we use this likelihood to reduce combinatorial background from random pions or physics backgrounds such as $D^+ \to K^-\pi^+\pi^+$. In [4], we vetoed D_s^+ candidates consistent with the D^+ mass hypothesis, which resulted in a substantial loss of signal efficiency. Kaon identification makes it possible to relax kinematic requirements (charged particle p_T and the D^+ veto) leading to a substantial increase in signal efficiency.

In the semileptonic channel, the main gain is in the $D_s^+\ell^-$, $D_s^+ \to \bar{K}^*(892)^0K^+$ sequence, where the signal is increased by a factor of 2.2. An additional gain in signal by a factor of 1.3 with respect to our previous analysis comes from adding data selected with different trigger requirements. In total the signal of 37 000 semileptonic B_s decays in [4] is increased to 61 500, and the signal to background improves by a factor of two in the sequences with kaons in the final state. The distributions of the invariant masses of the $D_s^+(\phi\pi^+)\ell^-$ pairs $m_{D_s\ell}$ and the $D_s^+(\phi\pi^+)$ candidates are shown in Fig. 1. We use $m_{D_s\ell}$ to help distinguish signal, which occurs at higher $m_{D_s\ell}$, from combinatorial and physics (*e.g.*, double-charm decays of B mesons) backgrounds.

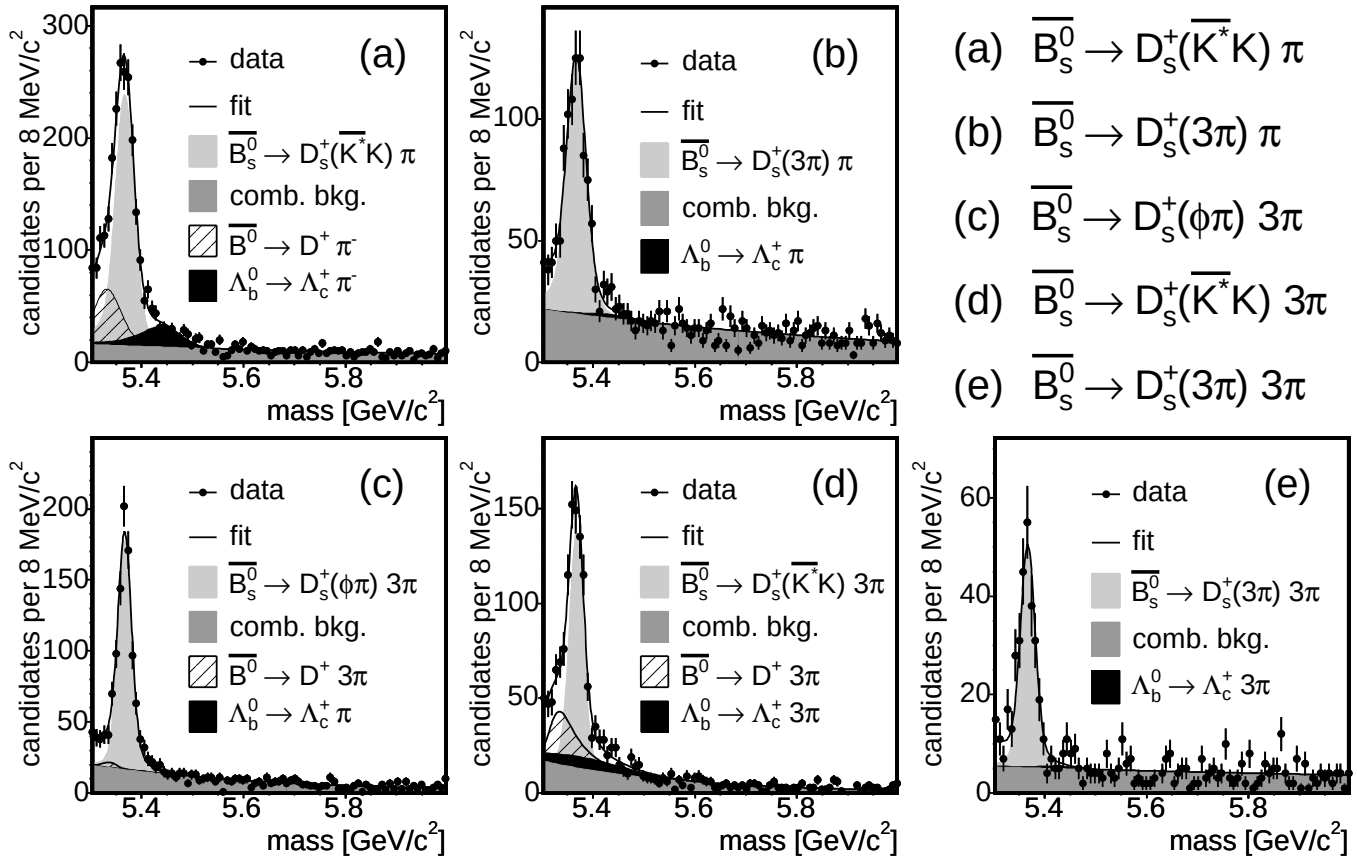

FIG. 2: The invariant mass distributions for $\bar{B}_s^0 \to D_s^+\pi^-$ (top panels) and $D_s^+\pi^-\pi^+\pi^-$ (bottom panels). Signal contributions are added on top of the combinatorial background. Contributions from partially reconstructed B_s decays are taken into account in the fit and are not shown.

In the hadronic decay modes, we use an ANN to enhance the signal selection of the previous analysis. The ANN uses quantities such as the selection criteria listed above as well as the kaon identification likelihood. The network is trained using simulated signals generated with Monte Carlo methods. For combinatorial background, we use sideband regions in the mass distribution of the B_s candidates from data. In this analysis, we add the partially reconstructed signal between 5.0 and 5.3 GeV/c^2 from $\bar{B}_s^0 \to D_s^{*+}\pi^-$, $D_s^{*+} \to D_s^+\gamma/\pi^0$ in which a photon or π^0 from the D_s^{*+} is missing and $\bar{B}_s^0 \to D_s^+\rho^-$, $\rho^- \to \pi^-\pi^0$ in which a π^0 is missing. The mass distributions for $\bar{B}_s^0 \to D_s^+\pi^-$, $D_s^+ \to \phi\pi^+$ and the partially reconstructed signals are shown in Fig. 1. The mass distributions for the other five hadronic decay

Decay Sequence	Signal	S/B	gain w.r.t [4]
$\bar{B}_s^0 \to D_s^+(\phi\pi^+)\pi^-$	2000	11.3	13%
Partially reconstructed	3100	3.4	n.a.
$\bar{B}_s^0 \to D_s^+(\bar{K}^*(892)^0K^+)\pi^-$	1400	2.0	35%
$\bar{B}_s^0 \to D_s^+(\pi^+\pi^-\pi^+)\pi^-$	700	2.1	22%
$\bar{B}_s^0 \to D_s^+(\phi\pi^+)\pi^-\pi^+\pi^-$	700	2.7	92%
$\bar{B}_s^0 \to D_s^+(\bar{K}^*(892)^0K^+)\pi^-\pi^+\pi^-$	600	1.1	110%
$\bar{B}_s^0 \to D_s^+(\pi^+\pi^-\pi^+)\pi^-\pi^+\pi^-$	200	2.6	n.a.

TABLE I: Signal yields (S) and signal to background ratio (S/B) in the various hadronic decay sequences. The gain refers to the percentage increase in $S/\sqrt{S+B}$ relative to [4].

sequences are shown in Fig. 2. In these modes, we require the masses of the candidates to be greater than $5.3\,\mathrm{GeV}/c^2$. Candidates with masses greater than $5.5\,\mathrm{GeV}/c^2$ are used to construct probability density functions (PDFs) for combinatorial background. Table I summarizes the signal yields.

The reconstructed decay time in the B_s rest frame is $t = m_{B_s}L_T/p_T^{\mathrm{recon}}$, where L_T is the displacement of the B_s decay point with respect to the primary vertex projected onto the B_s transverse momentum vector, and p_T^{recon} is the transverse momentum of the reconstructed decay products. In the semileptonic and partially reconstructed hadronic decays, we correct t by a factor $\kappa = p_T^{\mathrm{recon}}/p_T(B_s)$ determined with Monte Carlo simulation (Fig. 3).

The decay time resolution σ_t has contributions from the momentum of missing decay products (due to the spread of the distribution of κ) and from the uncertainty on L_T. The uncertainty due to the missing momentum increases with proper decay time and is an important contribution to σ_t in the semileptonic decays. To reduce this contribution and make optimal use of the semileptonic decays, we determine the κ distribution as a function of $m_{D_s\ell}$ (Fig. 3). We estimate the contribution from the uncertainty on L_T to σ_t for each candidate using the measured track parameters and their estimated uncertainties.

The distribution of σ_t for fully reconstructed decays has an average value of 87 fs, which corresponds to one fourth of an oscillation period at $\Delta m_s = 17.8\,\mathrm{ps}^{-1}$. The distribution is nearly Gaussian with an rms width of 31 fs. For the partially reconstructed hadronic decays, the average σ_t is 97 fs, and the addition to σ_t due to the missing photon or π^0 is very small (Fig. 3). For semileptonic decays, σ_t is worse due to decay topology and the much larger missing momentum of decay products that were not reconstructed. The increase of σ_t with t is illustrated in Fig. 3 for different ranges of $m_{D_s\ell}$.

The flavor of the B_s at production is determined using both opposite-side and same-side flavor tagging techniques. The effectiveness $Q \equiv \epsilon\mathcal{D}^2$ of these techniques is quantified with an efficiency ϵ, the fraction of signal candidates with a flavor tag, and a dilution $\mathcal{D} \equiv 1 - 2w$, where w is the probability that the tag is incorrect.

At the Tevatron, the dominant b-quark production mechanisms produce $b\bar{b}$ pairs. Opposite-side tags infer the production flavor of the B_s from the decay products of the b hadron produced from the other b quark in the event. In the previous analysis, we used lepton (e and μ) charge and jet charge as tags, and if both types of tag were present, we used the lepton tag. In this improved analysis, we add an opposite-side flavor tag based on the charge of identified kaons, and we combine the information from the kaon, lepton, and jet charge tags using an ANN. The dilution is measured in data [8] using large samples of B^-, which do not change flavor, and $\bar{B}^0$, which can be used after accounting for their well-known oscillation frequency. The combined opposite-side tag effectiveness improves by 20% to $Q = 1.8 \pm 0.1\,\%$. Most of the improvement is for candidates with both a lepton and jet-charge tag.

Same-side flavor tags are based on the charges of associated particles produced in the fragmentation of the b quark that produces the reconstructed B_s. In the previous analysis, we used a same-side tag based on our kaon particle-identification likelihood; here we use an ANN to combine our kaon particle-identification likelihood with kinematic quantities of the kaon candidate into a single tagging variable T. Tracks close in phase space to the B_s candidate are considered as same-side kaon tag candidates, and the track with the largest value of T is selected as the tagging track. We predict the dilution of the same-side tag using simulated data samples generated with the PYTHIA Monte Carlo [9] program. The predicted fractional gain in Q from using the ANN is 10%. Control samples of B^- and $\bar{B}^0$ are used to validate the predictions of the simulation. The effectiveness of this flavor tag increases with the p_T of the $\bar{B}_s^0$; we find $Q = 3.7\%$ (4.8%) in the hadronic (semileptonic) decay sample. The fractional uncertainty on Q is approximately 25% [4]. If both a same-side tag and an opposite-side tag are present, we combine the information from both tags assuming they are independent.

We use an unbinned maximum likelihood fit to search for B_s oscillations. The likelihood combines mass, decay

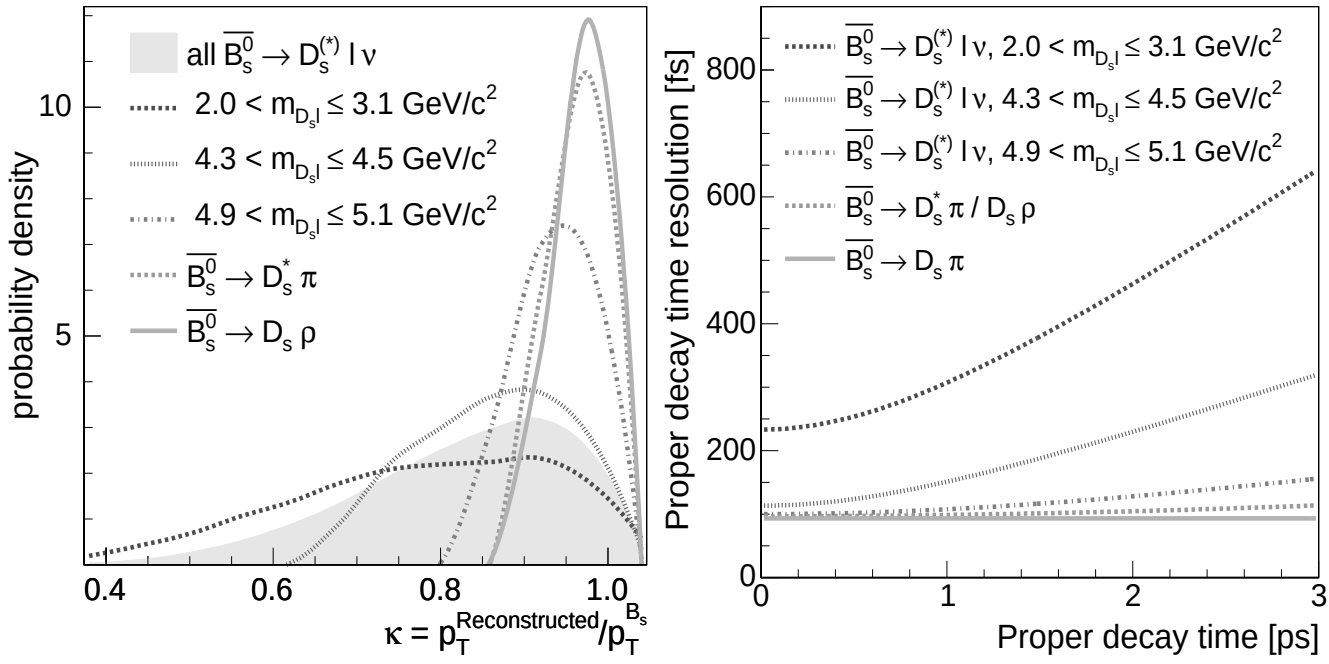

FIG. 3: (Left panel) The distribution of the correction factor κ in semileptonic and partially reconstructed hadronic decays from Monte Carlo simulation. (Right panel) The average proper decay time resolution for B_s decays as a function of proper decay time.

time, decay-time resolution, and flavor tagging information for each candidate, and includes terms for signal and each type of background. Details of the fit are described in [4, 10].

Following the method described in [11], we fit for the oscillation amplitude $\mathcal{A}$ while fixing Δm_s to a probe value. The oscillation amplitude is expected to be consistent with $\mathcal{A} = 1$ when the probe value is the true oscillation frequency, and consistent with $\mathcal{A} = 0$ when the probe value is far from the true oscillation frequency. Figure 4 shows the fitted value of the amplitude as a function of the oscillation frequency for the semileptonic candidates alone, the hadronic candidates alone, and the combination. The sensitivity [4, 11] is 19.3 ps^{-1} for the semileptonic decays alone, 30.7 ps^{-1} for the hadronic decays alone, and 31.3 ps^{-1} for all decays combined. At $\Delta m_s = 17.75$ ps^{-1}, the observed amplitude $\mathcal{A} = 1.21 \pm 0.20$ (stat.) is consistent with unity, indicating that the data are compatible with B_s^0-$\bar{B}_s^0$ oscillations with that frequency, while the amplitude is inconsistent with zero: $\mathcal{A}/\sigma_{\mathcal{A}} = 6.05$, where $\sigma_{\mathcal{A}}$ is the statistical uncertainty on $\mathcal{A}$ (the ratio has negligible systematic uncertainties). The small uncertainty on $\mathcal{A}$ at $\Delta m_s = 17.75$ ps^{-1} is due to the superior decay-time resolution of the hadronic decay modes.

We evaluate the significance of the signal using $\Lambda \equiv \log[\mathcal{L}^{\mathcal{A}=0}/\mathcal{L}^{\mathcal{A}=1}(\Delta m_s)]$, which is the logarithm of the ratio of likelihoods for the hypothesis of oscillations ($\mathcal{A} = 1$) at the probe value and the hypothesis that $\mathcal{A} = 0$, which is equivalent to random production flavor tags. Figure 4 shows Λ as a function of Δm_s. Separate curves are shown for the semileptonic data alone (dashed), the hadronic data alone (light solid), and the combined data (dark solid). At the minimum $\Delta m_s = 17.77$ ps^{-1}, $\Lambda = -17.26$. The significance of the signal is the probability that randomly tagged data would produce a value of Λ lower than -17.26 at any value of Δm_s. We repeat the likelihood scan 350 million times with random tagging decisions; 28 of these scans have $\Lambda < -17.26$, corresponding to a probability of 8×10^{-8} ($5.4\,\sigma$), well below 5.7×10^{-7} ($5\,\sigma$).

To measure Δm_s, we fix $\mathcal{A} = 1$ and fit for the oscillation frequency. We find $\Delta m_s = 17.77 \pm 0.10$ (stat) $\pm$ 0.07 (syst) ps^{-1}. The only non-negligible systematic uncertainty on Δm_s is from the uncertainty on the absolute scale of the decay-time measurement. Contributions to this uncertainty include biases in the primary-vertex reconstruction due to the presence of the opposite-side b hadron, uncertainties in the silicon-detector alignment, and biases in track fitting. The uncertainty on the correction κ for the hadronic candidates with a missing photon or π^0 is included and has a negligible effect.

The B_s^0-$\bar{B}_s^0$ oscillations are depicted in Fig. 5. Candidates in the hadronic sample are collected in five bins of proper decay time modulo the measured oscillation period $2\pi/\Delta m_s$. In each bin, we fit for an amplitude (the points in Fig. 5) using the likelihood function [4], which takes into account the effects of background, flavor tag dilution and

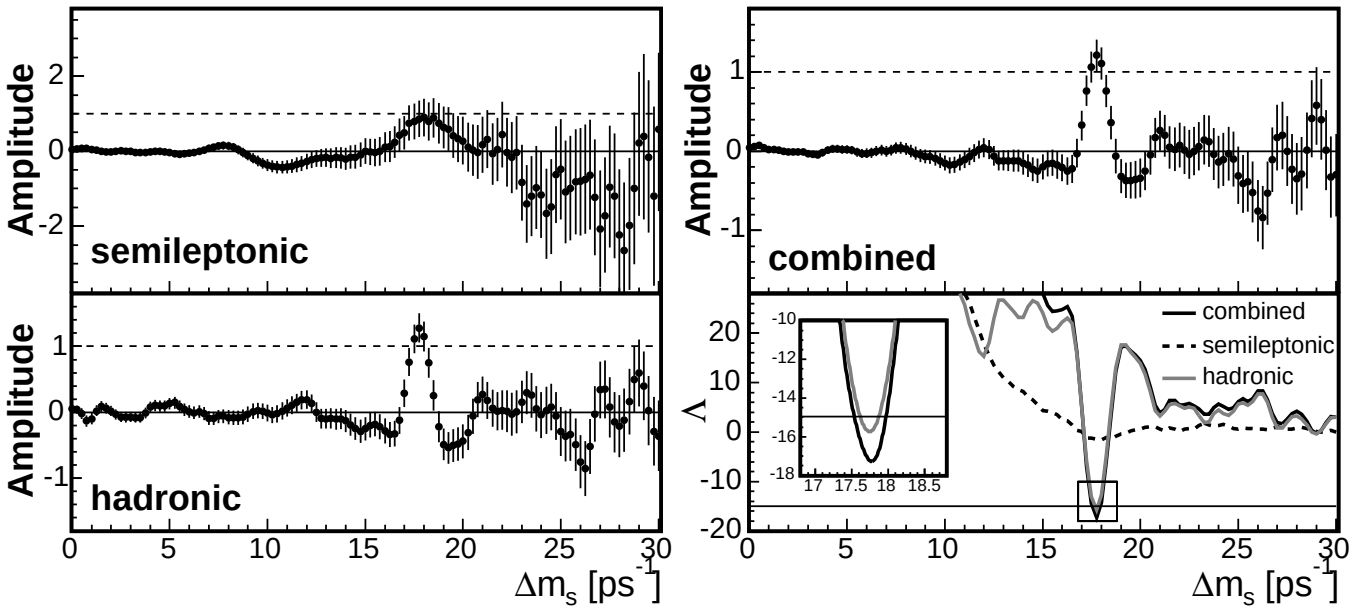

FIG. 4: The measured amplitude values and uncertainties versus the B_s^0-$\bar{B}_s^0$ oscillation frequency Δm_s. (Upper Left) Semileptonic decays only. (Lower Left) Hadronic decays only. (Upper Right) All decay modes combined. (Lower Right) The logarithm of the ratio of likelihoods for amplitude equal to one and amplitude equal to zero, $\Lambda = \log[\mathcal{L}^{\mathcal{A}=0}/\mathcal{L}^{\mathcal{A}=1}(\Delta m_s)]$, versus the oscillation frequency. The horizontal line indicates the value $\Lambda = -15$ that corresponds to a probability of 5.7×10^{-7} (5σ) in the case of randomly tagged data.

decay-time resolution for each candidate. The curve shown in Fig. 5 is a cosine with an amplitude of 1.28, which is the observed value in the amplitude scan for the hadronic sample at $\Delta m_s = 17.77\,\mathrm{ps}^{-1}$. As expected, the data are well represented by the curve.

The measured B_s^0-$\bar{B}_s^0$ oscillation frequency is used to derive the ratio $|V_{td}/V_{ts}| = \xi\sqrt{\frac{\Delta m_d}{\Delta m_s}\frac{m_{B_s^0}}{m_{B^0}}}$ [13]. As inputs we use $m_{B^0}/m_{B_s^0} = 0.98390$ [12] with negligible uncertainty, $\Delta m_d = 0.507 \pm 0.005\,\mathrm{ps}^{-1}$ [13] and $\xi = 1.21\ ^{+0.047}_{-0.035}$ [14]. We find $|V_{td}/V_{ts}| = 0.2060 \pm 0.0007\ (\mathrm{exp})\ ^{+0.0081}_{-0.0060}\ (\mathrm{theor})$.

In conclusion, we report the first observation of B_s^0-$\bar{B}_s^0$ oscillations from a decay-time dependent measurement of Δm_s. Our signal exceeds 5σ significance and yields a precise value of Δm_s, which is consistent with standard model expectations. This result supersedes our previous measurement [4].

We thank the Fermilab staff and the technical staffs of the participating institutions for their vital contributions. This work was supported by the U.S. Department of Energy and National Science Foundation; the Italian Istituto Nazionale di Fisica Nucleare; the Ministry of Education, Culture, Sports, Science and Technology of Japan; the Natural Sciences and Engineering Research Council of Canada; the National Science Council of the Republic of China; the Swiss National Science Foundation; the A.P. Sloan Foundation; the Bundesministerium für Bildung und Forschung, Germany; the Korean Science and Engineering Foundation and the Korean Research Foundation; the Particle Physics and Astronomy Research Council and the Royal Society, UK; the Institut National de Physique Nucleaire et Physique des Particules/CNRS; the Russian Foundation for Basic Research; the Comisión Interministerial de Ciencia y Tecnología, Spain; the European Community's Human Potential Programme under contract HPRN-CT-2002-00292; and the Academy of Finland.

[1] C. Albajar *et al.* (UA1 Collaboration) Phys. Lett. B **186**, 247 (1987); H. Albrecht *et al.* (ARGUS Collaboration) Phys. Lett. B **192**, 245 (1987).

[2] C. Gay, Annu. Rev. Nucl. Part. Sci. **50**, 577 (2000). Neutral B mesons ($b\bar{q}$, with $q = d, s$ for $\bar{B}^0$, $\bar{B}_s^0$) oscillate from particle to antiparticle due to flavor-changing weak interactions with a frequency proportional to the mass difference Δm_q between the two mass eigenstates $B_{q,H}^0$ and $B_{q,L}^0$. We set $\hbar = c = 1$ and report $\Delta m_s = m_{B_{s,H}^0} - m_{B_{s,L}^0}$ in inverse picoseconds.

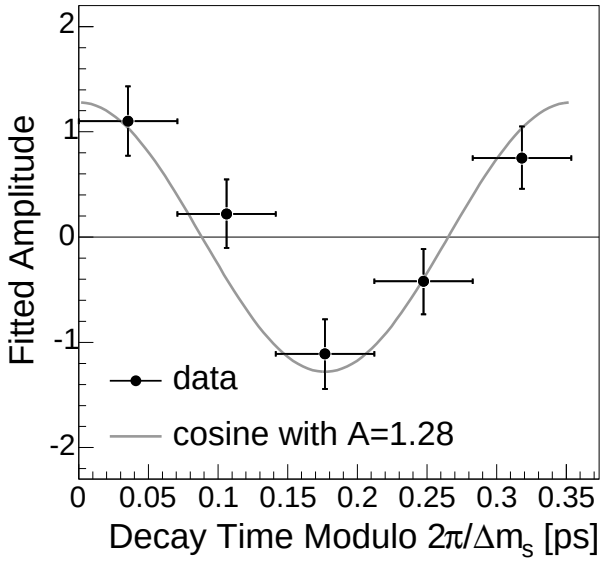

FIG. 5: The B_s^0-$\bar{B}_s^0$ oscillation signal measured in five bins of proper decay time modulo the measured oscillation period $2\pi/\Delta m_s$. The figure is described in the text.

[3] N. Cabibbo, Phys. Rev. Lett. **10**, 531 (1963); M. Kobayashi and T. Maskawa, Prog. Theor. Phys. **49**, 652 (1973).
[4] A. Abulencia *et al.* (CDF Collaboration), Phys. Rev. Lett. **97**, 062003 (2006).
[5] The symbol B_s refers to the combination of $\bar{B}_s^0$ and B_s^0 decays. References to a particular process imply that the charge conjugate process is included as well.
[6] D. Acosta *et al.* (CDF Collaboration), Phys. Rev. D **71**, 032001 (2005); R. Blair *et al.* (CDF Collaboration), Fermilab Report No. FERMILAB–PUB–96–390–E, 1996; C. S. Hill *et al.*, Nucl. Instrum. Methods Phys. Res., Sect. A **530**, 1 (2004); S. Cabrera *et al.*, Nucl. Instrum. Methods Phys. Res., Sect. A **494**, 416 (2002); W. Ashmanskas *et al.*, Nucl. Instrum. Methods Phys. Res., Sect. A **518**, 532 (2004).
[7] The transverse momentum p_T is the magnitude of the component of the momentum perpendicular to the proton beam direction.
[8] J. Piedra, Ph.D. thesis, University of Cantabria (Fermilab Report No. FERMILAB-THESIS-2005-27, 2005).
[9] T. Sjöstrand *et al.*, Computer Phys. Commun. **135**, 238 (2001). We use version 6.216.
[10] N. Leonardo, Ph.D. thesis, Massachusetts Institute of Technology (Fermilab Report No. FERMILAB-THESIS-2006-18, 2006).
[11] H. G. Moser and A. Roussarie, Nucl. Instrum. Methods Phys. Res., Sect. A **384**, 491 (1997).
[12] D. Acosta *et al.* (CDF Collaboration) Phys. Rev. Lett. **96**, 202001 (2006).
[13] W.-M. Yao *et al.* J. Phys. G **33**, 1 (2006).
[14] M. Okamoto, Proc. Sci. LAT2005 (2005) 013 [hep-lat/0510113].